Elimination of recalcitrant micropollutants by medium pressure UV-catalyzed bioelectrochemical advanced oxidation process

Influencing factors, transformation pathway and toxicity assessment

Zou, Rusen; Tang, Kai; Hambly, Adam C.; Chhetri, Ravi Kumar; Andersen, Henrik Rasmus; Zhang, Yifeng

Published in:
Science of the Total Environment

Link to article, DOI:
10.1016/j.scitotenv.2022.154543

Publication date:
2022

Document Version
Publisher's PDF, also known as Version of record

Science of the Total Environment 828 (2022) 154543

Contents lists available at ScienceDirect

Science of the Total Environment

journal homepage: www.elsevier.com/locate/scitotenv

Elimination of recalcitrant micropollutants by medium pressure UV-catalyzed bioelectrochemical advanced oxidation process: Influencing factors, transformation pathway and toxicity assessment

Rusen Zou, Kai Tang, Adam C. Hambly, Ravi Kumar Chhetri, Henrik Rasmus Andersen, Yifeng Zhang *

Department of Environmental Engineering, Technical University of Denmark, DK-2800 Lyngby, Denmark

HIGHLIGHTS

- Novel medium pressure UV-driven bioelectrochemical advanced oxidation process.
- The hybrid process was much faster than each individual one in removing pollutants.
- Reduced treatment cost compared to traditional processes (medium pressure UV/H_2O_2).
- Identified transformation pathways of model compounds during the hybrid process.
- It proved to be a promising way for removing micropollutants in secondary effluent.

GRAPHICAL ABSTRACT

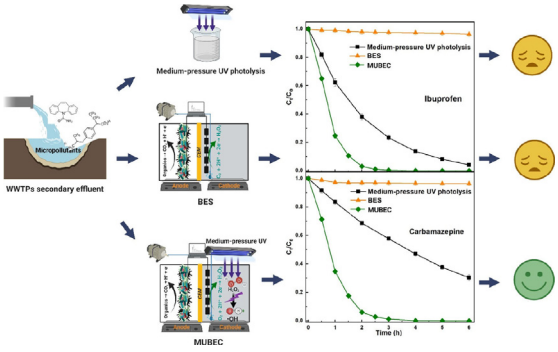

ARTICLE INFO

Article history:
Received 8 November 2021
Received in revised form 7 March 2022
Accepted 9 March 2022
Available online xxxx

Editor: Jorge de Brito

Keywords:
Micropollutants
Medium pressure UV
Bio-electro-Fenton
H_2O_2
Wastewater treatment
Ecotoxicity

ABSTRACT

Bio-electro-Fenton (BEF) processes have been widely studied in recent years to remove recalcitrant micropollutants from wastewater. Though promising, it still faces the critical challenge of residual iron and iron sludge in the treated effluent. Thus, an innovative medium-pressure ultraviolet-catalyzed bio-electrochemical system (MUBEC), in which medium-pressure ultraviolet was employed as an alternative to iron for in-situ H_2O_2 activation, was developed for the removal of recalcitrant micropollutants. The influence of operating parameters, including initial catholyte pH, cathodic aeration rate, and input voltage, on the system performance, was explored. Results indicated that complete reduction of 10 mg L^{-1} of model micro-pollutants ibuprofen (IBU) and carbamazepine (CBZ) was achieved at pH 3, with an aeration rate of 1 mL min^{-1} and a voltage of 0.3 V, following pseudo-first-order kinetics. Moreover, potential transformation pathways and the associated intermediates during the degradation were deduced and detected, respectively. Thus, the MUBEC system shows the potential for the efficient and cost-effective degradation of recalcitrant micropollutants from wastewater.

1. Introduction

In recent years, the appearance of micropollutants in water bodies worldwide has attracted increasing attention (Ribeiro et al., 2019; Schwarzenbach et al., 2006; Zhang et al., 2015a). Especially, trace pharmaceuticals are now commonly detected in wastewater treatment plant (WWTP) effluent and surface water, in concentrations from ng L^{-1} to μg L^{-1}. Ibuprofen (IBU) and carbamazepine (CBZ), as representative

* Corresponding author at: Department of Environmental Engineering, Technical University of Denmark, Denmark.
E-mail address: yifz@env.dtu.dk (Y. Zhang).

http://dx.doi.org/10.1016/j.scitotenv.2022.154543

pharmaceuticals, have been widely detected in water sources due to their extensive use and structural stability (Březinova et al., 2018; Naghdi et al., 2017). The ineffective treatment by conventional WWTP is likely their primary source, and they may have negative impacts on ecosystems and humans (Ao et al., 2018; Aymerich et al., 2016; Snyder et al., 2003). For example, the concentration of IBU detected in the influent of a WWTP in Spain reached 603 μg L^{-1} and its removal efficiency was only around 80% (Santos et al., 2009). In addition, it has been reported that the IBU removal efficiency of some WWTPs is as low as 7% (Letsinger et al., 2019). Accordingly, numerous studies have shown that IBU concentrations in the global water environment are much higher than other pharmaceuticals, up to about 6.3 μg L^{-1} (Oba et al., 2021). As a result of this continuous release into the environment, IBU has been identified as a common pharmaceuticals residue in WWTP effluent, sludge, and hospital wastewater, with detectable concentrations of up to 95 μg L^{-1}, 208 ng g^{-1}, and 92 μg L^{-1} in several European, American, and Asian countries, respectively (Ziylan and Ince, 2011; Luo et al., 2014; Zhou et al., 2018; Dubey et al., 2021). Further, Ekpeghere et al found that CBZ had the highest content in south Korean sewage treatment plants influent (maximum of 6.88 μg L^{-1}), and the removal efficiency was very low (usually less than 10%) (Ekpeghere et al., 2018). These pharmaceutical containing wastewaters, therefore, need to be further treated before discharge. So the development of an efficient technology for post-biological treatment in WWTPs has become a popular research topic.

Previous studies on the removal of trace pharmaceuticals from wastewater have so far mainly focused on advanced oxidation processes (AOPs), membrane filtration, and adsorption (Bonvin et al., 2016; Ribeiro et al., 2019; Taheran et al., 2016). In particular, electrochemical AOPs (e.g., the electro-Fenton process) have been considered promising technologies for degrading and mineralizing pharmaceuticals (Barhoumi et al., 2016; Feng et al., 2013; Monteil et al., 2019). Although the traditional electro-Fenton approaches have several advantages such as high efficiency, mild reaction conditions, and being environmentally friendly, major drawbacks such as the large electricity consumption and iron sludge generation still need to be addressed. In this context, a bio-electro Fenton (BEF) process has gained attention in recent years (Li et al., 2017b; Nadais et al., 2018; Zou et al., 2020a). BEF requires a much lower electricity input (0.2–0.8 V) as the anodic exoelectrogens can produce electrons for driving hydrogen peroxide (H_2O_2) production in the cathode. Currently, iron is widely studied as a catalyst to activate activate H_2O_2 for the production of hydroxyl radicals. However, it has several challenges for practical application. Firstly, adjustment of pH is required before and after the treatment (Li et al., 2018). Secondly, it is required to remove excess iron before discharge. Thirdly, the formation of iron sludge may affect treatment performance (Li et al., 2018). Thus, a new but cost-effective method is required to activate the in-situ generated H_2O_2 at the cathode. Ultraviolet (UV) radiation has been proven an alternative to the iron catalyst for H_2O_2 activation via Eq. (1) without the need for pH adjustment or iron sludge production.

$$H_2O_2 \xrightarrow{h\nu} 2 \cdot OH \quad (1)$$

UV-based AOPs such as the UV/H_2O_2 process has been widely used for wastewater treatment due to their distinct advantages over Fenton-based methods. In addition to solving the above problems, they also exhibit high H_2O_2 utilization and no secondary pollution (Swaim et al., 2008; Yang et al., 2017; Yuan et al., 2009). Low-pressure UV and medium-pressure UV lamps are two main types of light sources for the application. Among them, our earlier research by combining low-pressure UV with a bioelectrochemical system proved to be an environmentally friendly technology to remove micro-pollutants (e.g., carbamazepine) (Zou et al., 2020b). Compared to low-pressure UV, medium-pressure UV has an advantage of higher UVC intensity and thus could save reactor space (Ao et al., 2018; Pereira et al., 2007). Thus, medium-pressure UV could be an ideal alternative to iron in BEF. However, to the best of our knowledge, the integration of medium-pressure UV and BEF systems has not been reported.

In this work, an innovative medium-pressure ultraviolet-catalyzed bio-electrochemical system (MUBEC) was developed and investigated for micropollutants removal. Ibuprofen (IBU) and carbamazepine (CBZ) were chosen as model pharmaceuticals to evaluate the applicability of the novel process. The cathodic aeration rate, initial cathodic pH, and applied voltage were varied to study their effects on the efficiency of the treatment process. Besides, the degradation pathways of IBU and CBZ in MUBEC were studied. Moreover, the reaction intermediates were also identified. Furthermore, the effect of the water matrix on IBU and CBZ removal was investigated. Finally, an eco-toxicity test through *Vibrio fischeri* was conducted on the treated effluent to assess the bio-safety of this novel process. This work offers insights into developing viable microbial electrochemical advanced oxidation process for efficient and cost-effective removal of micropollutants from wastewater.

2. Materials and methods

2.1. MUBEC reactor construction and operation

A two-chamber (8 cm × 8 cm × 8 cm for each) lab-scale MUBEC reactor was constructed using cubic polycarbonate as previously described (Zou et al., 2022). Each chamber had an effective volume and a working volume of 218 mL and 200 mL, respectively. The anode chamber and cathode chamber were separated by a proton exchange membrane (Nafion 117, DuPont Co., USA). In the anode chamber, a carbon fiber brush (diameter 5.9 cm, length 6.9 cm, Mill-Rose, USA) was used as an electrode to enrich the biofilm. Further detail on the pre-treatment methods of the carbon fiber brush and the proton exchange membrane can be seen in previous studies (Jin et al., 2017; Zhang and Angelidaki, 2015). In the cathode chamber, the working electrode used a gas diffusion electrode with a projected size of 4 cm × 4 cm. The gas diffusion electrode was prepared as previously described (Yu et al., 2015). In addition, an Ag/AgCl electrode (+0.197 V vs SHE, Pine Instrument Company, USA) was placed in the cathode chamber as a reference electrode.

The startup of this MUBEC reactor followed the same methods as described in our previous study (Zou et al., 2020a). When a stable and repeatable voltage output (> 600 mV) was obtained in microbial fuel cell (MFC) mode, the reactor was supplied with external voltage and connected with a 10 Ω external resistor in the circuit. Domestic wastewater (influent picked up from Lyngby WWTP, Copenhagen, Denmark) spiked with 1 g L^{-1} sodium acetate anhydrous and 7.1 g L^{-1} sodium sulfate was used as the anolyte and catholyte, respectively. A peristaltic pump (BT100-2 J, Longer, China) was used for continuous aeration in the cathode chamber. A medium-pressure UV light (SR HUV700, 700W, Scan Research A/S, Denmark) with enhanced emission in the low wavelength region was used to irradiate the cathode chamber (shown in Fig. 1) (Hansen et al., 2013). The medium pressure UV lamp was operated for 30 min before each experiment to give a stable and repeatable light output. The distance between the UV lamp and the liquid level in the cathode chamber of the MEC reactor was 30 cm.

A proof-of-concept experiment was first conducted to evaluate the feasibility of this novel bioelectrochemical advanced oxidation process for the removal of selected model pharmaceuticals. After that, the impact of crucial operating parameters such as initial cathodic pH (3, 5, 6.8, 9, and 11), cathodic aeration rate (0, 1, 2, 4, and 8 mL min^{-1}), applied voltage (0.2, 0.3, 0.4, 0.5, 0.6, and 0.7 V) and water matrix (secondary biological treatment effluent collected from Lyngby WWTP, Copenhagen, Denmark) on system performance was explored. After sampling, 50 μL tert-butanol was added to the sample to quench the reaction. All experiments were performed in duplicate at room temperature (22 ± 5 °C).

2.2. Materials

Ibuprofen (IBU, CAS15687-27-1), carbamazepine (CBZ, CAS298-46-4), sodium sulfate, sodium acetate, H_2O_2 solution (30%, w/w), sulfuric acid,

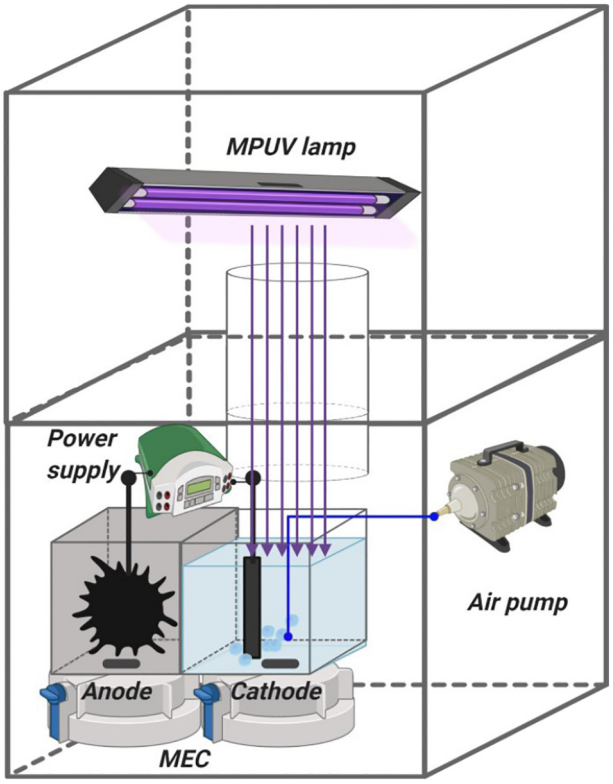

Fig. 1. Schematic diagram of MUBEC system setup.

sodium hydroxide, titanium potassium oxalate and tert-butanol were obtained from Sigma-Aldrich (Denmark). HPLC grade ethanol and acetonitrile were obtained from Merck (Germany). The solutions used in all experiments were prepared with deionized water, except for those used to study the degradation mechanism of IBU and CBZ. For the degradation mechanism experiments, MilliQ water was used to prepare the test solutions.

2.3. Analytical methods and calculations

The determination of the concentration of H_2O_2 was conducted in the same manner as described within our previous study (Nadais et al., 2018). A high-performance liquid chromatography (Agilent 1290 Infinity, USA, HPLC) system coupled with a tandem mass spectrometer (Agilent 6470 series, USA, MS/MS) was used to quantify the concentration of IBU and CBZ and to identify possible intermediates and construct a probable degradation mechanism. Specifically, full scans were performed in ESI negative and ESI positive modes, between 60 and 300 *m/z* to detect possible intermediate compounds. In combination with previously published literature, the most likely structures for the transformation products of IBU and CBZ in the MUBEC process could then be inferred. The detailed operational parameters of the HPLC/MS/MS system are shown in Text S1. The analytical methods used for solutions total organic carbon (TOC) and pH were the same as described in detail in our previous paper (Zou et al., 2020a). The system current (I) was calculated using Ohm's law (I = V/R), where both voltage (V) and cathode potential (V) data were collected via a digital multimeter (Model 2700, Keithley Instruments, Inc., Cleveland, OH, USA).

The behavior of applying ·OH based AOPs technologies to degrade pharmaceuticals is well known to be consistent with pseudo-first-order kinetics (Brillas et al., 2009). Hence, the apparent rate constant (Kapp) was calculated via Eq. (2).

$$K_{app}t = ln\frac{C_0}{C_t} \quad (2)$$

2.4. Eco-toxicity assays

The eco-toxicity assays of treated wastewater were determined by *Vibrio fischeri* bioluminescence inhibition experiment, where the details are described within a previous study (Tang et al., 2019). The experiment was performed using real wastewater spiked with IBU and CBZ at an initial concentration of 10 mg L^{-1}, respectively, and samples were obtained and analysed from throughout the 10-h reaction time (0, 0.5, 1, 1.5, 2, 2.5, 3, 4, 5, 6, 8, and 10 h).

3. Results and discussion

3.1. Proof-of-concept

Experiments were conducted to validate the feasibility of this novel MUBEC process for the removal of the selected model pharmaceuticals IBU (10 mg L^{-1}) and CBZ (10 mg L^{-1}). Also, the removal efficiencies of IBU and CBZ under different control experiments including adsorption, medium-pressure UV photolysis directly, MEC oxidation process alone, MUBEC (MFC mode) were compared. As shown in Fig. 2, the MUBEC

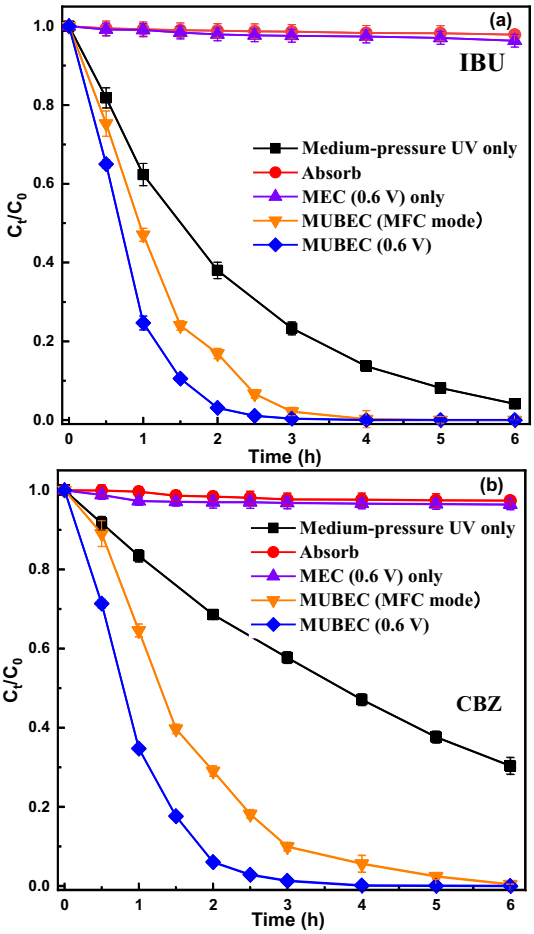

Fig. 2. Removal of IBU (a) and CBZ (b) through different treatment strategies. System operational parameters: initial IBU or CBZ of 10 mg L^{-1}, applied voltage of 0.6 V, aeration rate of 0.01 mL min^{-1} mL^{-1}, Na_2SO_4 of 50 mM, without pH adjustment and medium-pressure UV of 700 W.

system showed superior IBU and CBZ removal efficiency than that of each control experiment, reaching up to 99.9% and 100% for IBU and CBZ respectively, after 4 h of reaction time. By contrast, the MEC (0.6 V applied) oxidation process alone also exhibited negligible IBU and CBZ removal (less than 4% after 6 h). The result also indicates that the electrosynthesis of H_2O_2 can not oxidize the IBU and CBZ directly, which was in line with previous studies (Ghauch et al., 2011; Yuan et al., 2009). Furthermore, the results in Fig. 2 also show that both IBU and CBZ exhibited very low adsorption (less than 3% after 6 h), indicating that the effect of electrode adsorption on IBU and CBZ removal calculations is negligible. However, the UV light alone through photolysis showed high removal of IBU and CBZ (96% and 70%, respectively) after 6 h of irradiation. This is in contrast to previous UV irradiation studies that both IBU and CBZ were difficult to degrade under low-pressure UV direct photolysis (Kwon et al., 2015; Wang et al., 2016a; Wols et al., 2013). This difference can be attributed to the choice of lamp used, where medium-pressure UV lamp outputs polychromatic light across the range of 200 to 400 nm, while the low-pressure UV lamp outputs monochromatic light with a fixed wavelength of 254 nm (Ao et al., 2018; Shu et al., 2013). Moreover, the maximum absorption wavelength corresponding to IBU (220 nm) and CBZ (284 nm) is within the spectral range of 200 to 400 nm (Ao et al., 2018; Shu et al., 2013). The photodegradation of IBU and CBZ begins with medium-pressure UV irradiation of the photo-active aromatic rings in their molecular structures, generating IBU· and CBZ·in the active state, after which IBU· and CBZ· were further decomposed (Lu et al., 2018). Therefore, the improved IBU and CBZ removal efficiency during the MUBEC process was due to the protons and electrons generated by the anode of the MUBEC system, as they were transferred to the cathode chamber and then further reacted with oxygen molecules to create H_2O_2 via Eq. (3).

$$2H^+ + O_2 + 2e^- \rightarrow H_2O_2 \quad (3)$$

After that, the electrochemically synthesized H_2O_2 was further converted into·OH under medium pressure UV irradiation via Eq. (1). This radical generation is assumed to be the main reason behind the higher level of degradation of IBU and CBZ. Notably, the removal of IBU and CBZ under both medium-pressure UV direct irradiation and MUBEC process was consistent with pseudo-first-order kinetics, whereby the corresponding K_{app} values were 0.510 and 0.194 of IBU and 1.756 and 1.380 h^{-1} of CBZ under the above conditions, respectively. As such, the K_{app} values under the MUBEC process were 3.443 and 7.114 times the K_{app} values under medium-pressure UV direct irradiation conditions for IBU and CBZ, respectively. The results also indicate that the contribution of direct medium-pressure UV irradiation to the overall IBU and CBZ removal rate in the MUBEC system was low (29.1% and 4.1%, respectively). Furthermore, Fig. S1 shows the current and cathode potential recorded during the application of the MUBEC process, whereby the stable output of current and cathode potential reflected the stability of the system.

Overall, the above results demonstrated that the MUBEC process could effectively remove micropollutants from wastewater.

3.2. Influence of operating parameters on the MUBEC process for micropollutants removal

3.2.1. Influence of different catholyte pH

Several parameters could affect the micropollutants treatment in UV-based AOPs, such as UV/H_2O_2 and medium-pressure UV/H_2O_2 processes (Ao and Liu, 2017; Shemer and Linden, 2006). One such parameter is pH. Thus, the influence of catholyte pH (3, 5, 6.8, 9, and 11) on the degradation of IBU and CBZ was explored. As shown in Fig. 3, variation of the initial catholyte pH significantly affected the IBU and CBZ removal rates during the MUBEC process. Specifically, both removal rates declined significantly when the initial catholyte pH was increased from 3 to 5. After that, the removal rates showed a slow downward trend when the pH value was increased from 5 to 6.8 and further to 11. The above results were consistent with previous UV-based AOP studies (Ao and Liu, 2017; Elmolla and Chaudhuri, 2009; Naddeo et al., 2009). The main reasons for these results could be due to IBU dissociation (Iovino et al., 2016) and consumption of ·OH by the hydroperoxide anion (HO_2^-) generated via Eq. (4), and the self-decomposition of H_2O_2 under alkaline conditions via Eq. (5) (Deng et al., 2013). The reaction rate of HO_2^- with·OH was 100 times that with H_2O_2 via Eqs. (6) and (7) (Ao and Liu, 2017; Deng et al., 2013).

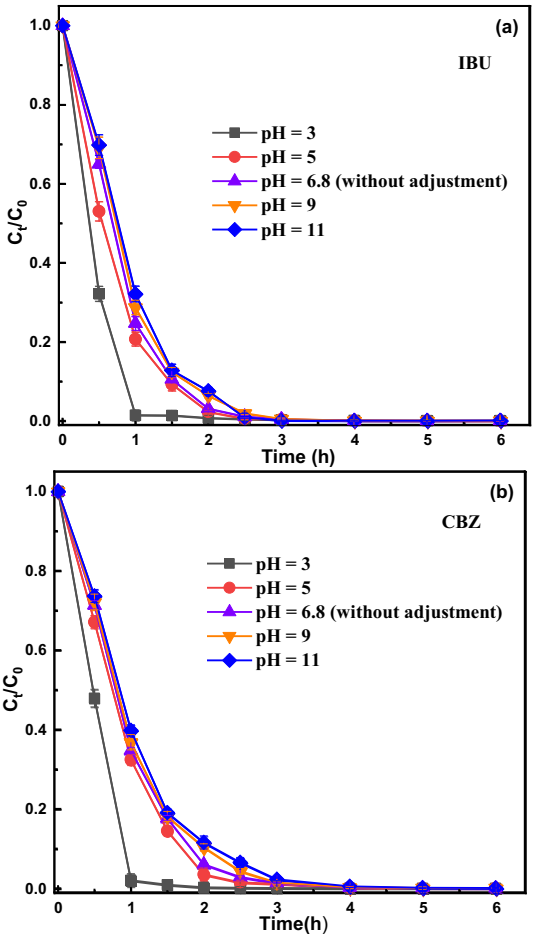

Fig. 3. Effect of initial catholyte pH on the removal of IBU (a) and CBZ (b) during the MUBEC process. System operational parameters: initial IBU or CBZ of 10 mg L^{-1}, applied voltage of 0.6 V, aeration rate of 0.01 mL min^{-1} mL^{-1}, Na_2SO_4 of 50 mM, and medium-pressure UV of 700 W.

$$H_2O_2 \leftrightarrow HO_2- + H^+ \quad (4)$$

$$2H_2O_2 \rightarrow 2H_2O + O_2 \quad (5)$$

$$\cdot OH + HO_2^- \rightarrow \cdot HO_2 + OH- \quad (6)$$

$$HO_2- + H_2O_2 \rightarrow H_2O + O_2 + OH^- \quad (7)$$

Moreover, since the pKa value of IBU was 4.85, the dissociation product of IBU in the negative ion state (IBU^-) will dominate as the pH value increased from 5 to 11, thereby improving the removal efficiency of IBU (Iovino et al., 2016). In addition, IBU will not dissociate when the pH is lower than 4.85. The CBZ existed as an electrically neutral substance throughout the whole pH range due to having a pKa of 14 (Maeng et al., 2015). Therefore, any variation in the initial catholyte pH would not affect the removal rate of CBZ under UV direct irradiation, which has also been observed in a previous study on the degradation of CBZ under UV direct irradiation (Maeng et al., 2015). Furthermore, the removal of IBU and CBZ under different initial catholyte pH was in line with the pseudo-first-order

kinetics. The K_{app} value with pH of 3, 5, 6.8, 9 and 11 were calculated to be 3.861, 1.900, 1.756, 1.576, 1.275 for IBU and 3.412, 1.457, 1.380, 1269, 1.050 h^{-1} for CBZ, respectively. The stable system current and cathode potential output (see in Fig. S2) indicated that the change of the catholyte pH did not affect the activity of the anode exoelectrogens.

Overall, the above results indicated that using medium-pressure UV (instead of iron) can overcome the problem of iron sludge production at pH above 4, thus allowing efficient micropollutant removal over a more wide pH range. In addition, the results also showed that the initial catholyte pH was a main influencing parameter that can significantly increase the removal rate under acidic conditions, thereby further reducing the cost of treating pharmaceutical-containing wastewater with the MUBEC process.

3.2.2. Influence of different cathodic aeration rates

Eq. (3) indicates that oxygen is one of the constituent elements for the in situ electrochemical syntheses of H_2O_2. Therefore, it is necessary to continuously pump air or pure oxygen to the cathode chamber to maintain dissolved oxygen saturation in the catholyte and reach the theoretical maximum yield of H_2O_2 (Labiadh et al., 2015). However, previous BEF studies on micropollutants treatment have shown that too high or low cathodic aeration rates would negatively affect system performance (Li et al., 2017b; Nadais et al., 2018; Zou et al., 2020a). In addition, the airflow rate needs to be controlled due to the use of a GDE cathode. This is required in order to maintain a pressure balance on both sides of GDE to avoid water leakage (Nishida et al., 2010).

In this section, five levels of cathodic aeration rates (0, 1, 2, 4, and 8 mL min^{-1}) were tested for the IBU and CBZ removal during the MUBEC process. Other experimental parameters included 10 mg L^{-1}initial IBU and CBZ concentrations, 0.6 V input voltage, 50 mM Na_2SO_4, and without any pH adjustment. As shown in Fig. 4, the removal rate of IBU and CBZ was firstly enhanced as the cathodic aeration rate increased from 0 to 1 mL min^{-1}, but then decreased as the cathodic aeration rates increased further from 1 to 2, 4 and eventually to 8 mL min^{-1}. The removal of IBU and CBZ under different cathodic aeration rates conformed to the pseudo-first-order kinetics, where the K_{app} values for IBU were 1.681, 1.944, 1.756, 1.471, 1.410 and for CBZ 1.336, 1.470, 1.380, 1.230, 1.228 h^{-1}, for 0, 1, 2, 4 and 8 mL min^{-1} respectively. Similar trends in K_{app} values have been obtained in previous studies on removing pharmaceuticals and dyes during the BEF process (Li et al., 2017b; Nadais et al., 2018; Zou et al., 2020a). The initial improvement in system performance when the cathodic aeration rate was raised from 0 to 1 mL min^{-1} could be attributed to the following. 1) the lack of oxygen supply resulted in lower H_2O_2 generation; and 2) faster mass transfer, manifested as reducing the rate of H_2O_2 migration from the GDE surface to the catholyte (Luo et al., 2015). In contrast, the lower K_{app} values were obtained when a higher cathodic aeration rate (above 1 mL min^{-1}) was applied, which can be due to 1) larger bubble sizes in contact with the GDE, thereby enhancing the catholyte resistance and reducing the probability of binding between the GDE active sites and the catholyte (Liu et al., 2007; Luo et al., 2015; Zhou et al., 2013); and 2) reduced UV radiation dose in UV-based AOPs (Moreira et al., 2017). Furthermore, the higher cathodic aeration rate will also increase power consumption and shorten the life of the air pump, thereby increasing treatment costs. The oxygen flow rates calculated from the cathodic aeration rate and the cathodic working volume ratio were 0, 0.0012, 0.0024, 0.0047, and 0.0093 mL O_2 min^{-1} mL^{-1}, and the optimum cathodic aeration rate was found to be 0.0024 mL O_2 min^{-1} mL^{-1}. This only accounted for 10–20% of the rates within previous BEF studies on the removal of pharmaceuticals and dyes (Nadais et al., 2018; Zhang et al., 2015b), and only 1% of the rate in previous EF studies on nitrotoluenes reduction (Chen and Lin, 2009). Due to the high efficiency of the MUBEF process, the reaction time was greatly shortened compared with previous BEF studies on the removal of IBU and CBZ (Nadais et al., 2018; Zou et al., 2020c), and the reactor, therefore, still showed good performance without aeration. The stable system current and cathode potential output can be seen in Fig. S3. The results show that scaling up the reactor and operating under continuous flow and aeration-free conditions is very feasible.

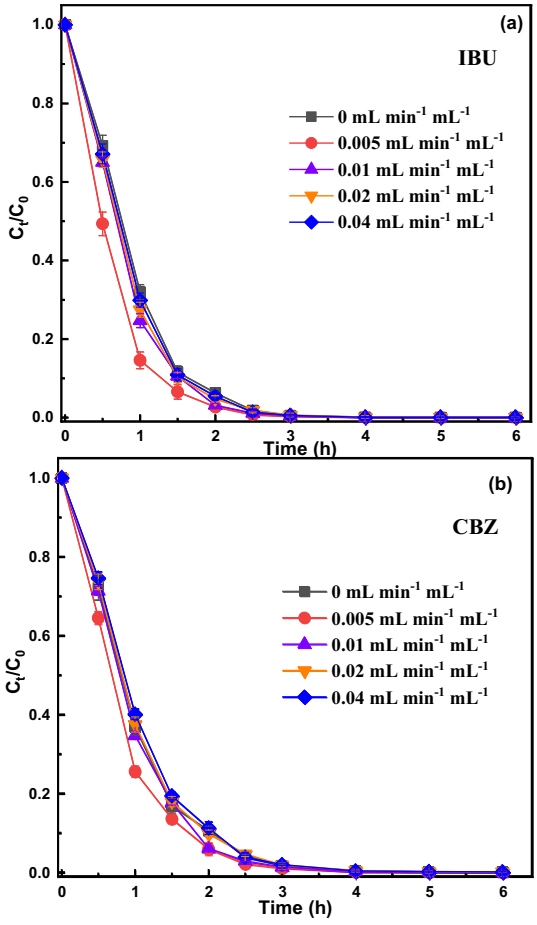

Fig. 4. Effect of cathodic aeration rates on the removal of IBU (a) and CBZ (b) during the MUBEC process. System operational parameters: initial IBU or CBZ of 10 mg L^{-1}, applied voltage of 0.6 V, Na_2SO_4 of 50 mM, without pH adjustment and medium-pressure UV of 700 W.

3.2.3. Influence of different applied voltages

The applied voltage is directly related to the amount of cathodic H_2O_2 synthesized via Eq. (3) (Brillas et al., 2009) and thus could be a crucial parameter to the MUBEC process performance. However, higher applied voltages do not represent higher pollutants removal efficiency. This is mainly because a higher applied voltage beyond the optimized value could promote side reactions, ultimately lowering system efficiency (Moreira et al., 2017). These known side reactions include 1) the depletion of ·OH and generation of H_2O_2 via Eq. (8), 2) the further conversion of electrosynthesised H_2O_2 into the water via Eq. (9), and 3) the further consumption of ·OH by excessive H_2O_2, to generate weakly oxidizable $HO_{\cdot 2}$ via Eq. (10) (Moreira et al., 2017).

$$2 \cdot OH \rightarrow H_2O_2 \quad (8)$$

$$2H^+ + H_2O_2 + 2e^- \rightarrow 2H_2O \quad (9)$$

$$\cdot OH + H_2O_2 \rightarrow H_2O + \cdot HO_2 \quad (10)$$

From an economic perspective, the higher applied voltage also leads to increased treatment costs. Thus, it is necessary to optimize the applied voltage to obtain efficient and cost-effective treatment of pollutants. In this section, applied voltages from 0.2 to 0.7 V as well as without any voltage input (reactor run in MFC mode)) were investigated. As shown in Fig. 5, the IBU and CBZ removal efficiency first increased significantly as the applied voltage increased from 0.2 to 0.3 V, but thereafter it decreased gradually as the applied voltage was increased from 0.3 to 0.7 V. The reasons for the adverse

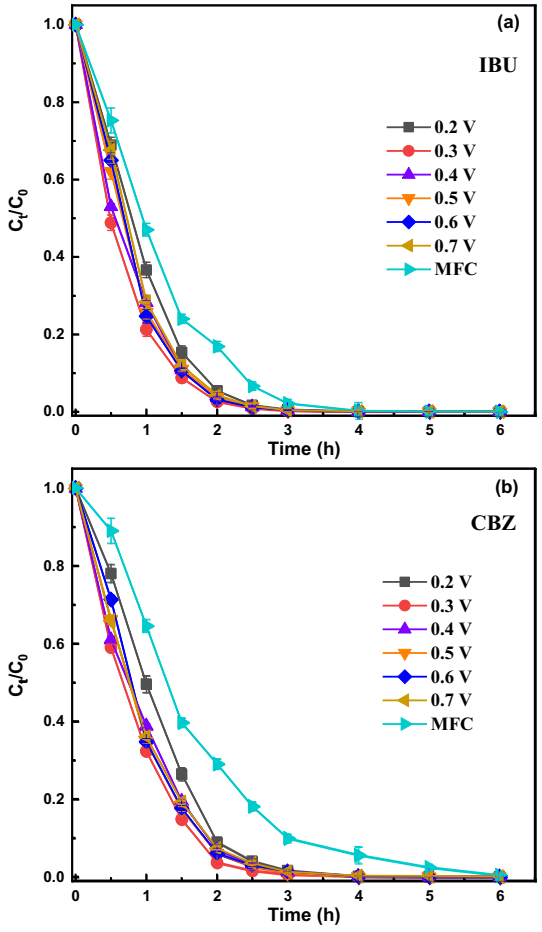

Fig. 5. Effect of applied voltage on the removal of IBU (a) and CBZ (b) during the MUBEC process. System operational parameters: initial IBU or CBZ of 10 mg L^{-1}, applied voltage of 0.6 V, aeration rate of 0.01 mL min^{-1} mL^{-1}, Na_2SO_4 of 50 mM, without pH adjustment and medium-pressure UV of 700 W.

effect of higher voltage input on the IBU and CBZ degradation could be attributed to the self-decomposition of H_2O_2 and ·OH via Eqs. (4), (6), and (7). Furthermore, at higher applied voltages, the rapid rise in pH could also cause the production of HO_2^- in the UV/H_2O_2 system, which eventually might consume the generated H_2O_2 and ·OH via Eqs. (4), (6), and (7) (Ao and Liu, 2017).

Fig. S4 shows the system current, cathode potential, and pH under various applied voltages conditions, whereby the current increases with the increase of the input voltage. Similar trends were seen in previous studies using the BEF process to treat dyes and aniline-containing wastewater (Li et al., 2017a; Zou et al., 2020a). Although the removal rate of the MUBEC process (MFC mode) was less than for the MUBEC process (MEC mode), IBU and CBZ were still removed with relatively high efficiency. Removals of IBU and CBZ were 98% and 90% at 3 h, respectively, which had increased to 100% and 99.7% at 6 h, respectively. This phenomenon could be explained by the much lower current (approx. 2 mA) in MFC mode leading to lower production of electrosynthesis H_2O_2 in the same time compared with that in MEC mode (4–12 mA). The removal of IBU and CBZ during the MUBEC process (MFC mode) with various applied voltages was also followed by pseudo-first-order kinetics. The K_{app} values in MFC mode corresponding to voltages of 0.2, 0.3, 0.4, 0.5, 0.6 and 0.7 V were 1.094, 1.573, 1.904, 1.743, 1.739, 1.756, 1.700 h^{-1} (IBU) and 0.683, 1.236, 1.451, 1.344, 1.435, 1.380, 1.340 h^{-1} (CBZ), which also showed the same trend as the removal rates. Previous studies have also attempted to remove 10 mg L^{-1} of CBZ using an MFC equipped with a FeMn catalyst-coated GDE. Although the CBZ treatment efficiency of this novel technology was superior to the traditional EF process (62% removal after 24 h) (Wang et al., 2018), but still 10% of CBZ was left after 24 h (Wang et al., 2018). The removal efficiency was still far lower than we observed with our MUBEC process, where both could remove more CBZ in much less time. In light of our results above, 0.3 V was selected as the optimal input voltage for removing IBU and CBZ during the MUBEC process.

3.2.4. Treatment cost calculation

The reactor was operated based on the optimal operating parameters observed from the above experiments. Notably, the MUBEC system was built to overcome the bottleneck that the BEF system can only operate under acidic conditions (pH of 2–4). As a result, Fig. 6 illustrates the removal effectiveness at acidic (pH of 3) as well as neutral circumstances (pH of 6.8). As seen in Fig. 6, full elimination of IBU and CBZ took 50 min or 2.5 h, depending on whether the system was operated under acidic or neutral conditions. In comparison to traditional EF and BEF technologies, the MUBEC process does not require the addition of iron as a catalyst and a broad operating pH range. So the overall treatment cost was predominantly due to electrical energy consumption. Specifically, the electrical energy consumption was mainly from two sources, including (1) the medium-pressure UV lamp (700 W) and (2) the MEC system including external voltage and pumping for aeration and agitation. To better compare the energy consumption in the MUBEC process with other treatment methods, the electrical energy per order (EE/O) was calculated. The details for this calculating method were described in Text S2, which is consistent

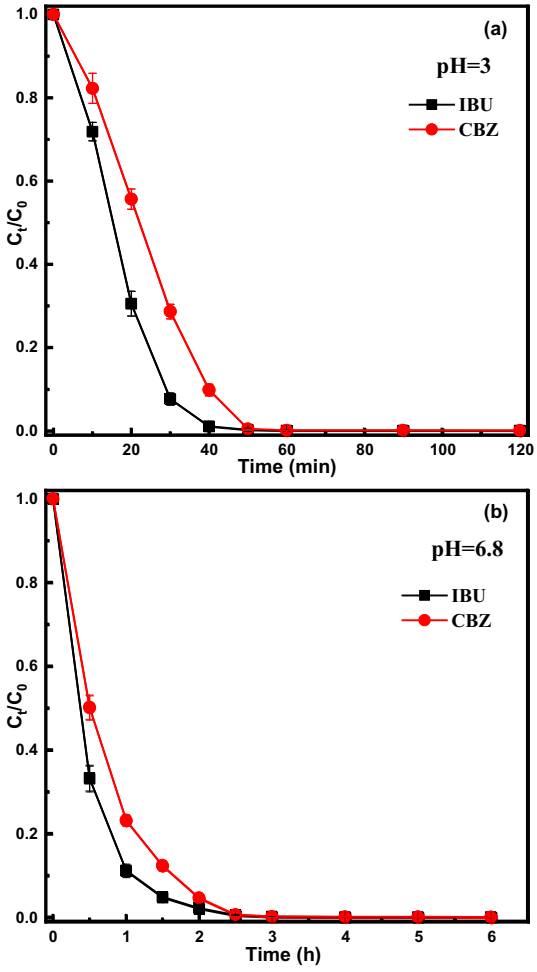

Fig. 6. Removal of IBU (a) and CBZ (b) during the MUBEC process under the optimal operating conditions. System operational parameters: initial IBU or CBZ of 10 mg L^{-1}, applied voltage of 0.3 V, aeration rate of 0.005 mL min^{-1} mL^{-1}, Na_2SO_4 of 50 mM, initial catholyte pH of 3 or without pH adjustment (pH of 6.8) and medium-pressure UV of 700 W.

Table 1
Economic analysis for the removal of pharmaceuticals during the MUBEC process.

Electrical energy-consuming components	EE/O (kWh m^{-3} $order^{-1}$)		Cost/O (€ m^{-3} $order^{-1}$)	
	pH = 3	pH = 6.8	pH = 3	pH = 6.8
Medium-pressure UV light	464.25	2187.50	60.35	284.38
Direct voltage supply	0.003	0.01	0.001	0.01
Cathodic aeration	1.33	6.25	0.17	0.81
Agitation	1.33	6.25	0.17	0.81
	466.91 (Total)	2200.01 (Total)	60.69 (Total)	286.00 (Total)

with previous studies (Pan et al., 2019; Shu et al., 2013). The electricity price in Denmark was quoted as 0.13 € per kWh. The correspondingly EE/O and cost per order (Cost/O) for the removal of IBU and CBZ under acidic and neutral conditions are shown in Table 1, respectively. The electrical energy consumption generated by the medium-pressure UV lamp accounts for about 99.5% of the total electrical energy consumption. The electrical energy consumption is compared with other methods for treating pharmaceuticals-containing wastewater (Table 2). From this, we can see the MUBEC process showed a faster removal rate and lower EE/O value when compared to the medium-pressure UV or ultrasound (US) based catalytic processes (e.g. medium-pressure UV/Fe(II) and US/PMS). When compared to the BEF process that was also derived from the MEC system, it is still in the same order of magnitude although the EE/O of the MUBEC process is higher. In contrast to BEF, the MUBEC process did not require the addition of iron as a catalyst and can operate efficiently over a more wide pH range. Furthermore, our previous research on MEC systems equipped with low-pressure UV lamps (MEUC system), presented a very low EE/O value on the treatment of CBZ-contaminated wastewater with a lower concentration (0.5 mg L^{-1}). It should be noted that this was only a proof-of-concept study and energy optimization is not carried out. Thus, a higher EE/O value could be expected. Specifically, it is equipped with a very powerful medium-pressure UV lamp (700 W), but only a small part of the UV radiation was effectively used. Nevertheless, it exhibits a much faster removal rate of pollutants than that of BEF and MEUC processes. Therefore, it can be expected that the volume of the MUBEC process reactor built will be smaller, and the corresponding capital and maintenance costs will be lower. The electrooxidation process using catalyst coated electrodes exhibits an order of magnitude lower E/EO value. However, the cost of catalyst preparation, recyclable times of catalyst and the feasibility of large-scale applications need to be considered. Finally, when compared with biodegradation processes (e.g., MFC) which require low or zero energy consumption, the MUBEC process shows a much greater pollutant removal rate. Therefore, MUBEC technology is a highly promising technology for rapid, efficient, and economical micropollutant removal.

3.3. Proposed IBU and CBZ degradation mechanism

LC-MS analyses were conducted to understand further the degradation mechanisms of IBU and CBZ in the MUBEC process. Correspondingly, the degradation pathways of IBU and CBZ were proposed as below.

3.3.1. Proposed transformation pathway of IBU

Fig. S5 shows the total ion chromatogram during the degradation of CBZ in the MUBEC process, where the elution time of transformation products appears at 2, 3.2–3.8, 4.1–4.8, 7.11, 9, and 9.4 min. The respective MS spectra corresponding to each of the highlighted elution times are shown in Fig. S6. The corresponding transformation products abundance trends with reaction time during the degradation of IBU in the MUBEC process can be seen in Fig. S7. Consequently, the corresponding transformation pathway of IBU is proposed in Fig. 7. Firstly, •OH produced by UV photocatalysis will attack different sites of IBU to create various mono-hydroxylated IBU with *m/z* 221.1 (TP1-1 to TP1-4), which has been previously detected in AOP-treatment studies (e.g., UV/PS and electro-peroxone processes) (Fu et al., 2019; Li et al., 2014). The transformation products with *m/z* 253 (TP2-1 to TP2-3) were most likely poly-hydroxy IBU, derived from mono-hydroxy IBU by a further reaction with •OH (Farhadi et al., 2020; Li et al., 2014). The •OH then attacked the side-chain sites of the above mono- or poly-hydroxy IBU, leading to decarboxylation or demethylation and the formation of aromatic intermediates with relatively low *m/z* (from 119 to 221.1) (Li et al., 2014; Xiang et al., 2016) . Structures TP1-5 and TP3-TP12 were then inferred from previous studies (e.g., solar radiation, photocatalysis and electrocatalytic processes) and listed in Fig. 7 (Arthur et al., 2018; Ding et al., 2019; Khalaf et al., 2020; Regmi et al., 2019; Rubasinghege et al., 2018; Wang et al., 2016b; Zhang et al., 2020). Finally, the benzene ring of the small-molecular aromatic transformation products

Table 2
Comparison of energy consumption on the removal of pharmaceuticals via different treatment technologies.

Treatment methods	Initial concentration (mg L^{-1})	Removal efficiency	Energy consumption (EE/O, kWh m^{-3})	References
Medium-pressure UV/H_2O_2 and medium-pressure UV/Fe(II) for CBZ removal	2	100% in 1.5 h (medium-pressure UV/H_2O_2) and 1 h (medium-pressure UV/ Fe(II))	576–9000	(Liu et al., 2015)
BEF process for IBU and 3 other NSAIDs removal	0.04 of each	Approx. 75% in 5 h	103.92	(Nadais et al., 2018)
Scaled-up BEF process for IBU, CBZ and 4 other pharmaceuticals removal	0.5 of each	100% in 18 h	162.21	(Zou et al., 2020a)
Photo (solar)-Fenton for pharmaceuticals (e.g., metoprolol) removal	50	90% in 1 h	1033	(Romero et al., 2016)
MEUC for CBZ removal	0.5	94% in 1 h and 98% in 2 h	6.07	(Zou et al., 2020b)
Electro-oxidation process using Ti/PbO_2 and Ti/BDD anodes	10	Approx. 82% in 101 min and 89% in 2 h	44 (Ti/PbO_2) and 40 (Ti/BDD)	(García-Gómez et al., 2014)
Ultrasound based H_2O_2, PS and PMS process for IBU removal	5	Approx. 50%–62.5% in 1 h	263.5–554.2	(Lee et al., 2020)
Ultrasound based PMS process for pharmaceuticals (e.g. sulfamethazine) removal	50	100% in 30 min	1510	(Yin et al., 2018)
MFC for CBZ removal	0.05	80% in 24 h	–	(Werner et al., 2015)
Rotating biological contactors for CBZ removal	0.02	85% in 240 h	–	(Vasiliadou et al., 2014)
Biological sludge system for IBU removal	0.1	100% in 36 h	–	(Jia et al., 2020)
MUBEC process for the IBU and CBZ removal	10 of each	100% in 50 min (pH of 3) and 100% in 2.5 h (pH of 6.8)	466.91 (pH of 3) and 2200.01 (pH of 6.8)	In this study

– Not mentioned in the paper.

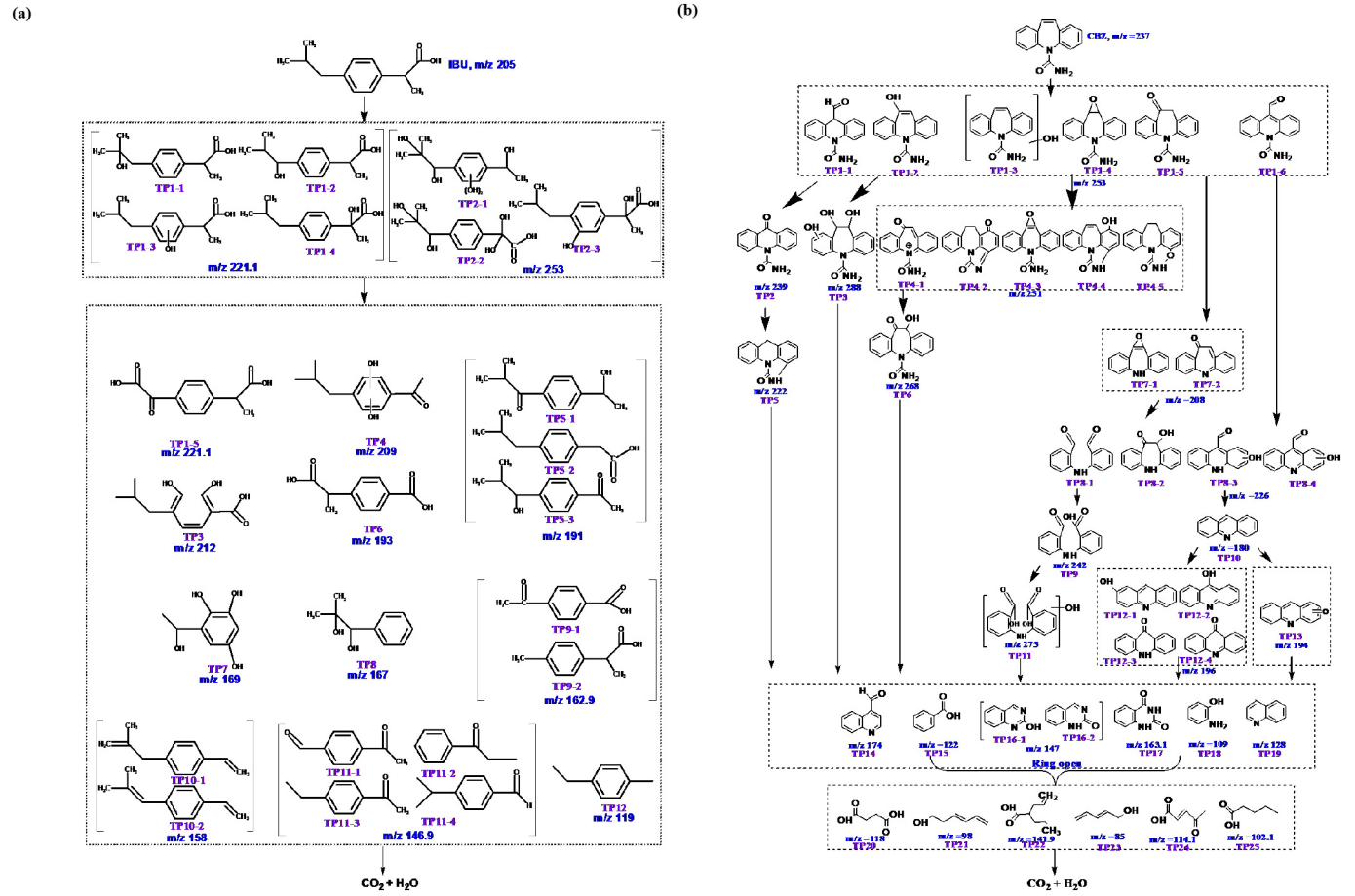

Fig. 7. The proposed transformation pathway of IBU (a) and CBZ (b) during the MUBEC process.

produced above were hydroxylated, resulting in ring cleavage and generation of short-chain carbohydrates (not detected), whereafter complete mineralization could occur (Bo et al., 2017).

3.3.2. Proposed transformation pathway of CBZ

All intermediate products and parent CBZ were eventually completely removed as the reaction progressed, demonstrating the mineralization ability of the MUBEC technology for these pollutants. Regardless, transformation products were still identified, and a likely transformation pathway of CBZ could therefore be proposed (Fig. 7) Fig. S8 showed eight elution times of the transformation products, at 2.25, 2.95, 5.2, 5.3 5.75, 8.2, 8.8, and 9.95 min. The respective MS spectra corresponding to each of the highlighted elution times during the degradation of CBZ in the MUBEC process are shown in Fig. S9. The corresponding transformation products abundance trends with reaction time during the degradation of CBZ in the MUBEC process can be seen in Fig. S10. As shown in Fig. 7, ·OH first combines with the N-containing heterocyclic or aromatic ring sites of the parent CBZ through an addition reaction to form monohydroxy CBZ (*m/z* 253). This is a common transformation product found in previous CBZ studies that have observed six possible different molecular structures (TP1-1 to TP1-6) (Bo et al., 2017; Franz et al., 2020; Wang et al., 2016a). Among these structures, TP1-1 and TP1-6 were formed by further ring contraction. The resulting monohydroxy CBZ was probably further oxidized by hydroxyl radicals through the following reactions. (1) TP1-1 is converted to TP2-1 and TP2-2 (*m/z* 239) through the loss of aldehyde group, then further converted to TP5 (*m/z* 222) through the formation of an intramolecular ring (Franz et al., 2020). (2) TP1-2 generates TP3 (*m/z* 288) through an addition reaction (Wang and Wang, 2017). (3) monohydroxy CBZ may involve intramolecular reactions to generate a transformation product with an *m/z* of 251, with 5 possible structures (TP4-1 to TP4-5) (Bessa et al., 2019; Sun et al., 2013; Wang and Wang, 2017; Wang et al., 2016a). (4) monohydroxy CBZ further reacts with·OH causing the loss of amide groups to produce transformation products TP7-1 and TP7-2 (*m/z* 208) (Jelic et al., 2013; Wang and Wang, 2018). Of these, TP9-3 and TP9-4 (*m/z* 226) derived from TP1-6 have also been found in UV/H_2O_2 process treating CBZ (Lu and Hu, 2019). Furthermore, the transformation product with *m/z* of 226 may have two other structures (TP9-1 and TP9-2), caused by ·OH attacking the aromatic rings of TP7-1 and TP7-2 (Jelic et al., 2013; Wu et al., 2019). With the continuous generation of ·OH within the system, intermediate TP8-1 can be oxidized to intermediate TP9 (*m/z* 242) or a complex hydroxylated intermediate TP12 (*m/z* 275) (Kråkström et al., 2020; Xu et al., 2013). The intermediates (*m/z* 226) can react with ·OH resulting in the loss of -CHO and -CO functional groups or addition of hydroxyl groups to generate intermediates with *m/z* 180 (TP11), 194 (TP15-1 and TP15-2), and 196 (TP14-1 to TP14-4) (Bo et al., 2017; Lu and Hu, 2019; Zhu et al., 2019). These transformation products then undergo hydroxylation of the aromatic ring, leading to ring cleavage (TP16-TP22) and complete ring-opening to generate small molecular hydrocarbons (TP23-TP29) (Bo et al., 2017; Gao et al., 2015; Moztahida et al., 2019). Finally, the produced small molecular hydrocarbons were completely mineralized, as confirmed by the mass spectra.

3.4. Matrix effects of WWTP secondary effluent

As discussed in the introduction, traditional WWTPs have great difficulty in removing micro-pollutants. Thus, emerging AOPs such as EF and UV/H_2O_2 have been used in recent years as a tertiary treatment process after WWTPs secondary biological treatment. The interaction between AOPs and the vast amount of compounds found within WWTP secondary effluent has been previously observed (Nadais et al., 2018; Zou et al.,

2020a) It can potentially decrease the performance of our MUBEC treatment process. Thus, the influence of the water matrix on the removal of IBU and CBZ during the MUBEC process was investigated. The detailed characteristics of the secondary biological treatment effluent are detailed in Table S1. Notably, the actual secondary biological treatment effluent was used here, and the conductivity is significantly lower than the previous pure water with the addition of 7 g L^{-1} sodium sulfate as the electrolyte (782 μs cm^{-1} vs 7450 μs cm^{-1}). As a result, the MUBEC has a lower current (see Fig. S11) when treating the actual wastewater at the same voltage (0.3 V) applied to synthetic wastewater, which means that less H_2O_2 is generated, ultimately leading to the generation of fewer ·OH. Therefore, we further boosted the current by increasing the voltage, which increased the production of H_2O_2 and even ·OH. When further increased to 0.7 V, the system's current at this point was comparable to the current at 0.3 V when treating synthetic wastewater. Therefore, we chose three voltage gradients of 0.3 0.5 and 0.7 V in this section. The experimental parameters were 10 mg L^{-1} initial IBU and CBZ concentrations, 1 mL min^{-1} mL^{-1} cathodic aeration rate, and 0.3, 0.5, and 0.7 V input voltages. Fig. 8 shows that in the effluent matrix, the complete removal of IBU and CBZ took up to 9 h without pH adjustment. It was a marked decrease in performance compared to pure water, which only required 2.5 h to achieve the same result. Despite the added wastewater matrix, the process still followed pseudo-first-order kinetics. The K_{app} values of IBU and CBZ for the real effluent under the three input voltages (0.3, 0.5 and 0.7 V) were 1.062, 0.624, 0.571 respectively for IBU and 0.561, 0.337, 0.326 respectively for CBZ. Notably, these values were from 62% to 78% lower than was observed in a pure water matrix. The results are likely due to the following. 1) natural organic matter (NOM) in the real effluent matrix absorbed part of the UV light and hence led to a decrease in the conversion efficiency of H_2O_2 to ·OH (Ribeiro et al., 2019). 2) the NOM directly participated in the reaction with ·OH, reducing the number of ·OH that react with target micro-pollutants. 3) the presence of inorganic ions (CO_3^{2-}, HCO_3^-, Cl^-, NO_3^-). Among the inorganic ions, CO_3^{2-} and HCO_3^- can scavenge the ·OH via Eqs. (11) and (12) and lead to the lower removal efficiency of IBU and CBZ (Ao and Liu, 2017; Ribeiro et al., 2019). In contrast, the presence of NO_3^- enhances the removal efficiency of micropollutants, especially in medium-pressure UV-based systems, where medium-pressure UV light with wavelengths between 200 nm and 300 nm induces significant NO3-photolysis, leading to the formation of a large number of ·OH system via Eq. (13) (Ao and Liu, 2017). Medium-pressure UV radiation with wavelengths less than 250 nm, in particular, promotes strong NO_3^- photolysis (Ao and Liu, 2017). Cl^- has a negligible impact on the rate of oxidation of organic contaminants during the MUBEC system, as although Cl^- can react with ·OH to form $ClHO^-$·via Eq. (14), $ClHO^-$·has also been shown to decompose into·OH rapidly (Zhang et al., 2018).

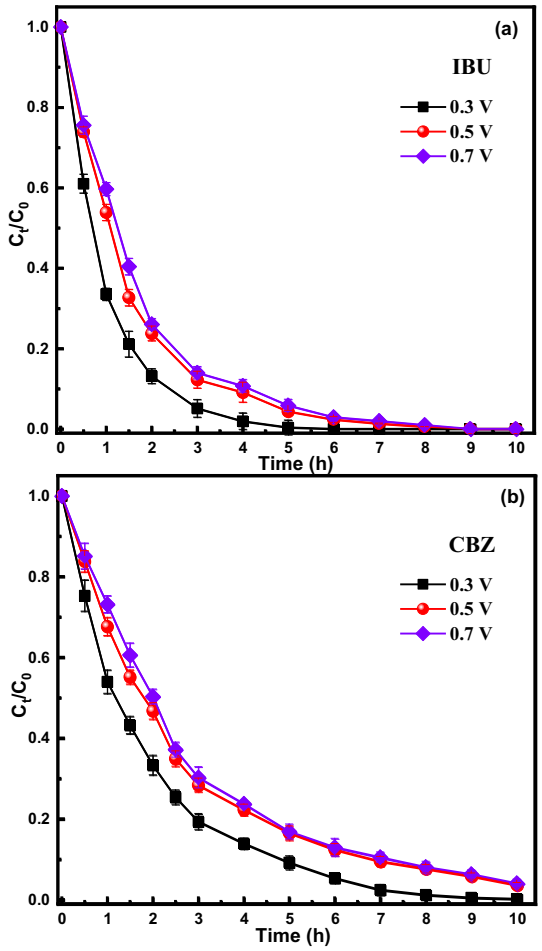

Fig. 8. Applicability of the MUBEC process on the removal of IBU (a) and CBZ (b) in a real WWTPs secondary effluent. System operational parameters: initial IBU or CBZ of 10 mg L^{-1}, applied voltage of 0.3, 0.5 and 0.7 V, aeration rate of 0.005 mL min^{-1} mL^{-1}, without pH adjustment, and medium-pressure UV of 700 W.

$$\cdot OH + CO_3^{2-} \rightarrow OH- + CO_3^{-}\cdot \quad (11)$$

$$\cdot OH + HCO_3^{-} \rightarrow H_2O + CO_3^{-}\cdot \quad (12)$$

$$NO_3- + H_2O \xrightarrow{h\nu} \cdot OH + NO_2\cdot + OH- \quad (13)$$

$$\cdot OH + Cl^- \rightarrow ClHO^-\cdot \quad (14)$$

Similar behavior was also found in previous studies on both BEF and (MP)UV/H_2O_2 removal of micropollutants (Ao et al., 2018; Nadais et al., 2018; Zhang et al., 2018). In light of the defects of the water matrix on the removal efficiency of micropollutants and subsequent increased treatment costs, the mechanism between its components and the formation of multiple species with oxidizing capacity should be further studied in the future, to maximize the treatment performance of this novel technology.

3.5. Ecotoxicity assessment

Although MUBEC technology had been found to have sound mineralization effects on IBU and CBZ, it required a longer reaction time. It resulted in greater energy consumption than is needed by simply removing the precursors of IBU and CBZ. Notably, the discharge of treated effluent potentially containing reaction intermediates may have a negative impact on the ecology of natural aquatic systems. Therefore, microtox assays were conducted to assess the ecotoxicity of the samples described in Section 3.4. Precisely, the potential ecological toxicity could be estimated by adding *Vibrio fischeri* to the samples and observing the variation of their luminescence inhibition rates (%) after exposure time at 10 and 20 min. As shown in Fig. 9, the luminous inhibition rate of *Vibrio fischeri* only slightly fluctuated throughout the whole reaction process, and there was no significant change compared with the control group. In addition, the luminous inhibition rates were all less than 20% in both the control group and the experimental group. The result indicates that the treated effluent was not significantly ecologically toxic (Zou et al., 2020b). In contrast, previous studies have found significant ecotoxicity due to direct UV photolysis or visible light-induced treatment process for the treatment of CBZ (Donner et al., 2013). The results indicate the improved environmental friendliness of our MUBEC technology. It should be emphasized that the concentrations of IBU and CBZ used in our study were significantly higher than what is typically seen in environmental samples. In practice, the concentration of transformation products produced during the treatment process will be lower, as will any of the associated risks.

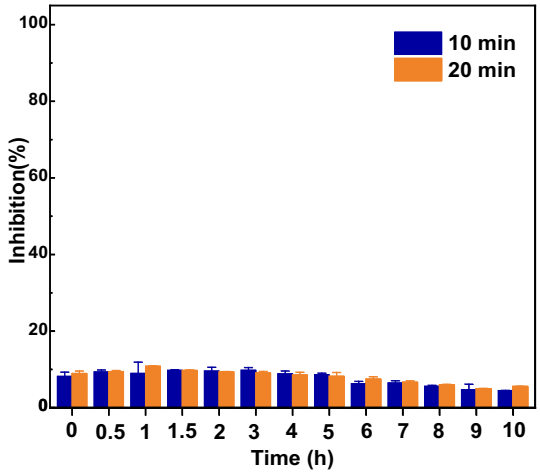

Fig. 9. Assess eco-toxicity of the treated effluent by measuring the luminescence inhibition rate (%) of *Vibrio fischeri* at two assay times (10 and 20 min). System operational parameters: initial IBU or CBZ of 10 mg L^{-1}, applied voltage of 0.3 V, aeration rate of 0.005 mL min^{-1} mL^{-1}, without pH adjustment, and medium-pressure UV of 700 W.

3.6. Implications

This study firstly demonstrated the feasibility and application of a unique MUBEC system to eliminate the recalcitrant micropollutants from WWTP secondary effluent efficiently. Compared to conventional UV-based AOPs (such as UV/H_2O_2) and the newly developed BEF and MEUC systems, the MUBEC system offers significant benefits in terms of treatment efficiency, cost, and the ability to treat at a broader working pH range. While the results are encouraging, the following issues should be addressed before field implementation. Firstly, the low conductivity in real wastewater could be the key challenge for practical application. The conductivity issue could be addressed by combining two different wastewaters of varying conductivity (Zou et al., 2020c). Secondly, the salt load will require further treatment if pH adjustment is needed before discharge (i.e., the pH rises dramatically with a longer run duration). In this case, the application of additional membranes, such as reverse osmosis membranes, would be required, which would lead to overall cost efficiency issues. Recently, bipolar membranes have been shown in earlier BEF investigations to be an excellent ion separator, preventing pH increases in the cathodic chamber and pH decreases in the anodic chamber (Li et al., 2017a). Thus, bipolar membranes can be utilized in the future to maintain pH in MUBEC systems, thus avoiding pH adjustment or reducing the acid-base consumed to adjust pH.

4. Conclusions

In this study, an innovative MUBEC process was developed and shown to remove model micro-pollutants IBU and CBZ effectively by integrating an emerging BEF with medium pressure UV. Under optimal operating conditions (0.3 V voltage, cathodic aeration rate of 1 mL min^{-1} and pH 3), 10 mg L^{-1} of IBU and CBZ were completely removed within 50 min, which is much faster than BEF, medium pressure UV/H_2O_2, MEUC and other biological processes (e.g., MFC). The MUBEC process has much broader working pH range than typical EF and BEF processes. Economic calculations indicate that the MUBEC process can reduce operating costs on the removal of micropollutants compared to medium pressure UV/H_2O_2 technology. In addition, the transformation intermediates of IBU and CBZ were determined and the corresponding pathways were proposed, respectively, in which ring opening, contraction and hydroxylation were the main ways. Finally, it was shown that wastewater matrices could have an inhibitory effect on system performance due to the radicals scavenging by NOM and inorganic ions (e.g., CO_3^{2-} and HCO_3^-). Considering all of the above, the MUBEC process is a promising technology that could be applied for the tertiary treatment of WWTPs to remove recalcitrant micropollutants.

CRediT authorship contribution statement

Rusen Zou: designed the methodology, conducted the experiments, and wrote the original manuscript. **Kai Tang:** contributed to the chemical analysis and edited the manuscript. **Adam C. Hambly:** contributed to the resources and the visualization. **Ravi Kumar Chhetri**: contributed to the resources. **Henrik Rasmus Andersen:** contributed to the resources and the visualization. **Yifeng Zhang:** conceptualization, experiment design, methodology, Funding acquisition and edited the manuscript.

Declaration of competing interest

The authors declare that they have no known competing financial interests or personal relationships that could have appeared to influence the work reported in this paper.

Acknowledgments

The authors would like to acknowledge the China Scholarship Council for their financial support. Yifeng Zhang thanks The Carlsberg Foundation for awarding The Carlsberg Foundation Distinguished Fellowships (CF18-0084).

Appendix A. Supplementary data

Supplementary data to this article can be found online at https://doi.org/10.1016/j.scitotenv.2022.154543.

References

Ao, X., Liu, W., 2017. Degradation of sulfamethoxazole by medium pressure UV and oxidants: peroxymonosulfate, persulfate, and hydrogen peroxide. Chem. Eng. J. 313, 629–637.
Ao, X., Liu, W., Sun, W., Cai, M., Ye, Z., Yang, C., Lu, Z., Li, C., 2018. Medium pressure UV-activated peroxymonosulfate for ciprofloxacin degradation: kinetics, mechanism, and genotoxicity. Chem. Eng. J. 345, 87–97.
Arthur, R.B., Bonin, J.L., Ardill, L.P., Rourk, E.J., Patterson, H.H., Stemmler, E.A., 2018. Photocatalytic degradation of ibuprofen over BiOCl nanosheets with identification of intermediates. J. Hazard. Mater. 358, 1–9.
Aymerich, I., Acuña, V., Barceló, D., García, M., Petrovic, M., Poch, M., Rodriguez-Mozaz, S., Rodríguez-Roda, I., Sabater, S., von Schiller, D., 2016. Attenuation of pharmaceuticals and their transformation products in a wastewater treatment plant and its receiving river ecosystem. Water Res. 100, 126–136.
Barhoumi, N., Oturan, N., Olvera-Vargas, H., Brillas, E., Gadri, A., Ammar, S., Oturan, M.A., 2016. Pyrite as a sustainable catalyst in electro-Fenton process for improving oxidation of sulfamethazine. Kinetics, mechanism and toxicity assessment. Water Res. 94, 52–61.
Bessa, V.S., Moreira, I.S., Murgolo, S., Mascolo, G., Castro, P.M., 2019. Carbamazepine is degraded by the bacterial strain labrys portucalensis F11. Sci. Total Environ. 690, 739–747.
Bo, L., He, K., Tan, N., Gao, B., Feng, Q., Liu, J., Wang, L., 2017. Photocatalytic oxidation of trace carbamazepine in aqueous solution by visible-light-driven Znln2S4: performance and mechanism. J. Environ. Manag. 190, 259–265.
Bonvin, F., Jost, L., Randin, L., Bonvin, E., Kohn, T., 2016. Super-fine powdered activated carbon (SPAC) for efficient removal of micropollutants from wastewater treatment plant effluent. Water Res. 90, 90–99.
Březinova, T.D., Vymazal, J., Koželuh, M., Kule, L., 2018. Occurrence and removal of ibuprofen and its metabolites in full-scale constructed wetlands treating municipal wastewater. Ecol. Eng. 120, 1–5.
Brillas, E., Sirés, I., Oturan, M.A., 2009. Electro-Fenton process and related electrochemical technologies based on Fenton's reaction chemistry. Chem. Rev. 109 (12), 6570–6631.
Chen, W.-S., Lin, S.-Z., 2009. Destruction of nitrotoluenes in wastewater by electro-Fenton oxidation. J. Hazard. Mater. 168 (2–3), 1562–1568.
Deng, J., Shao, Y., Gao, N., Xia, S., Tan, C., Zhou, S., Hu, X., 2013. Degradation of the antiepileptic drug carbamazepine upon different UV-based advanced oxidation processes in water. Chem. Eng. J. 222, 150–158.
Ding, Y., Nie, W., Li, W., Chang, Q., 2019. Co-doped NaBiO3 nanosheets with surface confined co species: high catalytic activation of peroxymonosulfate and ultra-low co leaching. Chem. Eng. J. 356, 359–370.
Donner, E., Kosjek, T., Qualmann, S., Kusk, K.O., Heath, E., Revitt, D.M., Ledin, A., Andersen, H.R., 2013. Ecotoxicity of carbamazepine and its UV photolysis transformation products. Sci. Total Environ. 443, 870–876.

Dubey, M., Mohapatra, S., Tyagi, V.K., Suthar, S., Kazmi, A.A., 2021. Occurrence, fate, and persistence of emerging micropollutants in sewage sludge treatment. Environ. Pollut. 273, 116515.

Ekpeghere, K.I., Sim, W.-J., Lee, H.-J., Oh, J.-E., 2018. Occurrence and distribution of carbamazepine, nicotine, estrogenic compounds, and their transformation products in wastewater from various treatment plants and the aquatic environment. Sci. Total Environ. 640, 1015–1023.

Elmolla, E., Chaudhuri, M., 2009. Optimization of Fenton process for treatment of amoxicillin, ampicillin and cloxacillin antibiotics in aqueous solution. J. Hazard. Mater. 170 (2–3), 666–672.

Farhadi, N., Tabatabaie, T., Ramavandi, B., Amiri, F., 2020. Optimization and characterization of zeolite-titanate for ibuprofen elimination by sonication/hydrogen peroxide/ultraviolet activity. Ultrason. Sonochem. 67, 105122.

Feng, L., Van Hullebusch, E.D., Rodrigo, M.A., Esposito, G., Oturan, M.A., 2013. Removal of residual anti-inflammatory and analgesic pharmaceuticals from aqueous systems by electrochemical advanced oxidation processes. A review. Chem. Eng. J. 228, 944–964.

Franz, S., Falletta, E., Arab, H., Murgolo, S., Bestetti, M., Mascolo, G., 2020. Degradation of carbamazepine by photo (electro) catalysis on nanostructured TiO2 meshes: transformation products and reaction pathways. Catalysts 10 (2), 169.

Fu, Y., Gao, X., Geng, J., Li, S., Wu, G., Ren, H., 2019. Degradation of three nonsteroidal anti-inflammatory drugs by UV/persulfate: degradation mechanisms, efficiency in effluents disposal. Chem. Eng. J. 356, 1032–1041.

Gao, X., Zhang, X., Wang, Y., Peng, S., Yue, B., Fan, C., 2015. Photocatalytic degradation of carbamazepine using hierarchical BiOCl microspheres: some key operating parameters, degradation intermediates and reaction pathway. Chem. Eng. J. 273, 156–165.

García-Gómez, C., Drogui, P., Zaviska, F., Seyhi, B., Gortáres-Moroyoqui, P., Buelna, G., Neira-Sáenz, C., Estrada-Alvarado, M., Ulloa-Mercado, R., 2014. Experimental design methodology applied to electrochemical oxidation of carbamazepine using Ti/PbO_2 and Ti/BDD electrodes. J. Electroanal. Chem. 732, 1–10.

Ghauch, A., Baydoun, H., Dermesropian, P., 2011. Degradation of aqueous carbamazepine in ultrasonic/Fe0/H2O2 systems. Chem. Eng. J. 172 (1), 18–27.

Hansen, K.M., Zortea, R., Piketty, A., Vega, S.R., Andersen, H.R., 2013. Photolytic removal of DBPs by medium pressure UV in swimming pool water. Sci. Total Environ. 443, 850–856.

Iovino, P., Chianese, S., Canzano, S., Prisciandaro, M., Musmarra, D., 2016. Degradation of ibuprofen in aqueous solution with UV light: the effect of reactor volume and pH. Water Air Soil Pollut. 227 (6), 194.

Jelic, A., Michael, I., Achilleos, A., Hapeshi, E., Lambropoulou, D., Perez, S., Petrovic, M., Fatta-Kassinos, D., Barcelo, D., 2013. Transformation products and reaction pathways of carbamazepine during photocatalytic and sonophotocatalytic treatment. J. Hazard. Mater. 263, 177–186.

Jia, Y., Yin, L., Khanal, S.K., Zhang, H., Oberoi, A.S., Lu, H., 2020. Biotransformation of ibuprofen in biological sludge systems: investigation of performance and mechanisms. Water Res. 170, 115303.

Jin, X., Li, X., Zhao, N., Angelidaki, I., Zhang, Y., 2017. Bio-electrolytic sensor for rapid monitoring of volatile fatty acids in anaerobic digestion process. Water Res. 111, 74–80.

Khalaf, S., Shoqeir, J.H., Lelario, F., Bufo, S.A., Karaman, R., Scrano, L., 2020. TiO2 and active coated glass photodegradation of ibuprofen. Catalysts 10 (5), 560.

Kråkström, M., Saeid, S., Tolvanen, P., Kumar, N., Salmi, T., Kronberg, L., Eklund, P., 2020. Ozonation of carbamazepine and its main transformation products: product determination and reaction mechanisms. Environ. Sci. Pollut. Res. 1–12.

Kwon, M., Kim, S., Yoon, Y., Jung, Y., Hwang, T.-M., Lee, J., Kang, J.-W., 2015. Comparative evaluation of ibuprofen removal by UV/H2O2 and UV/S2O82− processes for wastewater treatment. Chem. Eng. J. 269, 379–390.

Labiadh, L., Oturan, M.A., Panizza, M., Hamadi, N.B., Ammar, S., 2015. Complete removal of AHPS synthetic dye from water using new electro-Fenton oxidation catalyzed by natural pyrite as heterogeneous catalyst. J. Hazard. Mater. 297, 34–41.

Lee, Y., Lee, S., Cui, M., Ren, Y., Park, B., Ma, J., Han, Z., Khim, J., 2020. Activation of peroxodisulfate and peroxymonosulfate by ultrasound with different frequencies: impact on ibuprofen removal efficient, cost estimation and energy analysis. Chem. Eng. J. 127487.

Letsinger, S., Kay, P., Rodríguez-Mozaz, S., Villagrassa, M., Barceló, D., Rotchell, J.M., 2019. Spatial and temporal occurrence of pharmaceuticals in UK estuaries. Sci. Total Environ. 678, 74–84.

Li, X., Wang, Y., Yuan, S., Li, Z., Wang, B., Huang, J., Deng, S., Yu, G., 2014. Degradation of the anti-inflammatory drug ibuprofen by electro-peroxone process. Water Res. 63, 81–93.

Li, X., Jin, X., Zhao, N., Angelidaki, I., Zhang, Y., 2017a. Efficient treatment of aniline containing wastewater in bipolar membrane microbial electrolysis cell-Fenton system. Water Res. 119, 67–72.

Li, X., Jin, X., Zhao, N., Angelidaki, I., Zhang, Y., 2017b. Novel bio-electro-Fenton technology for azo dye wastewater treatment using microbial reverse-electrodialysis electrolysis cell. Bioresour. Technol. 228, 322–329.

Li, X., Chen, S., Angelidaki, I., Zhang, Y., 2018. Bio-electro-Fenton processes for wastewater treatment: advances and prospects. Chem. Eng. J. 354, 492–506.

Liu, H., Wang, C., Li, X., Xuan, X., Jiang, C., Cui, H.N., 2007. A novel electro-Fenton process for water treatment: reaction-controlled pH adjustment and performance assessment. Environ. Sci. Technol. 41 (8), 2937–2942.

Liu, N., Sijak, S., Zheng, M., Tang, L., Xu, G., Wu, M., 2015. Aquatic photolysis of florfenicol and thiamphenicol under direct UV irradiation, UV/H2O2 and UV/Fe (II) processes. Chem. Eng. J. 260, 826–834.

Lu, G., Hu, J., 2019. Effect of alpha-hydroxy acids on transformation products formation and degradation mechanisms of carbamazepine by UV/H2O2 process. Sci. Total Environ. 689, 70–78.

Lu, X., Shao, Y., Gao, N., Chen, J., Deng, H., Chu, W., An, N., Peng, F., 2018. Investigation of clofibric acid removal by UV/persulfate and UV/chlorine processes: kinetics and formation of disinfection byproducts during subsequent chlor (am) ination. Chem. Eng. J. 331, 364–371.

Luo, Y., Guo, W., Ngo, H.H., Nghiem, L.D., Hai, F.I., Zhang, J., Liang, S., Wang, X.C., 2014. A review on the occurrence of micropollutants in the aquatic environment and their fate and removal during wastewater treatment. Sci. Total Environ. 473, 619–641.

Luo, H., Li, C., Wu, C., Zheng, W., Dong, X., 2015. Electrochemical degradation of phenol by in situ electro-generated and electro-activated hydrogen peroxide using an improved gas diffusion cathode. Electrochim. Acta 186, 486–493.

Maeng, S.K., Cho, K., Jeong, B., Lee, J., Lee, Y., Lee, C., Choi, K.J., Hong, S.W., 2015. Substrate-immobilized electrospun TiO2 nanofibers for photocatalytic degradation of pharmaceuticals: the effects of pH and dissolved organic matter characteristics. Water Res. 86, 25–34.

Monteil, H., Péchaud, Y., Oturan, N., Oturan, M.A., 2019. A review on efficiency and cost effectiveness of electro-and bio-electro-Fenton processes: application to the treatment of pharmaceutical pollutants in water. Chem. Eng. J. 376, 119577.

Moreira, F.C., Boaventura, R.A., Brillas, E., Vilar, V.J., 2017. Electrochemical advanced oxidation processes: a review on their application to synthetic and real wastewaters. Appl. Catal. B Environ. 202, 217–261.

Moztahida, M., Jang, J., Nawaz, M., Lim, S.-R., Lee, D.S., 2019. Effect of rGO loading on Fe3O4: a visible light assisted catalyst material for carbamazepine degradation. Sci. Total Environ. 667, 741–750.

Nadais, H., Li, X., Alves, N., Couras, C., Andersen, H.R., Angelidaki, I., Zhang, Y., 2018. Bio-electro-Fenton process for the degradation of non-steroidal anti-inflammatory drugs in wastewater. Chem. Eng. J. 338, 401–410.

Naddeo, V., Meriç, S., Kassinos, D., Belgiorno, V., Guida, M., 2009. Fate of pharmaceuticals in contaminated urban wastewater effluent under ultrasonic irradiation. Water Res. 43 (16), 4019–4027.

Naghdi, M., Taheran, M., Brar, S.K., Kermanshahi-pour, A., Verma, M., Surampalli, R.Y., 2017. Immobilized laccase on oxygen functionalized nanobiochars through mineral acids treatment for removal of carbamazepine. Sci. Total Environ. 584, 393–401.

Nishida, K., Murakami, T., Tsushima, S., Hirai, S., 2010. Measurement of liquid water content in cathode gas diffusion electrode of polymer electrolyte fuel cell. J. Power Sources 195 (11), 3365–3373.

Oba, S.N., Ighalo, J.O., Aniagor, C.O., Igwegbe, C.A., 2021. Removal of ibuprofen from aqueous media by adsorption: a comprehensive review. Sci. Total Environ. 780, 146608.

Pan, Y., Zhang, Y., Zhou, M., Cai, J., Tian, Y., 2019. Enhanced removal of emerging contaminants using persulfate activated by UV and pre-magnetized Fe0. Chem. Eng. J. 361, 908–918.

Pereira, V.J., Linden, K.G., Weinberg, H.S., 2007. Evaluation of UV irradiation for photolytic and oxidative degradation of pharmaceutical compounds in water. Water Res. 41 (19), 4413–4423.

Regmi, C., Kshetri, Y.K., Kim, T.-H., Dhakal, D., Lee, S.W., 2019. Mechanistic understanding of enhanced photocatalytic activity of N-doped BiVO4 towards degradation of ibuprofen: an experimental and theoretical approach. Mol. Catal. 470, 8–18.

Ribeiro, A.R.L., Moreira, N.F., Puma, G.L., Silva, A.M., 2019. Impact of water matrix on the removal of micropollutants by advanced oxidation technologies. Chem. Eng. J. 363, 155–173.

Romero, V., González, O., Bayarri, B., Marco, P., Giménez, J., Esplugas, S., 2016. Degradation of Metoprolol by photo-Fenton: comparison of different photoreactors performance. Chem. Eng. J. 283, 639–648.

Rubasinghege, G., Gurung, R., Rijal, H., Maldonado-Torres, S., Chan, A., Acharya, S., Rogelj, S., Piyasena, M., 2018. Abiotic degradation and environmental toxicity of ibuprofen: roles of mineral particles and solar radiation. Water Res. 131, 22–32.

Santos, J., Aparicio, I., Callejón, M., Alonso, E., 2009. Occurrence of pharmaceutically active compounds during 1-year period in wastewaters from four wastewater treatment plants in Seville (Spain). J. Hazard. Mater. 164 (2–3), 1509–1516.

Schwarzenbach, R.P., Escher, B.I., Fenner, K., Hofstetter, T.B., Johnson, C.A., Von Gunten, U., Wehrli, B., 2006. The challenge of micropollutants in aquatic systems. Science 313 (5790), 1072–1077.

Shemer, H., Linden, K.G., 2006. Degradation and by-product formation of diazinon in water during UV and UV/H2O2 treatment. J. Hazard. Mater. 136 (3), 553–559.

Shu, Z., Bolton, J.R., Belosevic, M., El Din, M.G., 2013. Photodegradation of emerging micropollutants using the medium-pressure UV/H2O2 advanced oxidation process. Water Res. 47 (8), 2881–2889.

Snyder, S.A., Westerhoff, P., Yoon, Y., Sedlak, D.L., 2003. Pharmaceuticals, personal care products, and endocrine disruptors in water: implications for the water industry. Environ. Eng. Sci. 20 (5), 449–469.

Sun, S.-P., Zeng, X., Lemley, A.T., 2013. Kinetics and mechanism of carbamazepine degradation by a modified Fenton-like reaction with ferric-nitrilotriacetate complexes. J. Hazard. Mater. 252, 155–165.

Swaim, P., Royce, A., Smith, T., Maloney, T., Ehlen, D., Carter, B., 2008. Effectiveness of UV advanced oxidation for destruction of micro-pollutants. Ozone Sci. Eng. 30 (1), 34–42.

Taheran, M., Brar, S.K., Verma, M., Surampalli, R.Y., Zhang, T.C., Valéro, J.R., 2016. Membrane processes for removal of pharmaceutically active compounds (PhACs) from water and wastewaters. Sci. Total Environ. 547, 60–77.

Tang, K., Spiliotopoulou, A., Chhetri, R.K., Ooi, G.T., Kaarsholm, K.M., Sundmark, K., Florian, B., Kragelund, C., Bester, K., Andersen, H.R., 2019. Removal of pharmaceuticals, toxicity and natural fluorescence through the ozonation of biologically-treated hospital wastewater, with further polishing via a suspended biofilm. Chem. Eng. J. 359, 321–330.

Wang, S., Wang, J., 2017. Carbamazepine degradation by gamma irradiation coupled to biological treatment. J. Hazard. Mater. 321, 639–646.

Wang, S., Wang, J., 2018. Degradation of carbamazepine by radiation-induced activation of peroxymonosulfate. Chem. Eng. J. 336, 595–601.

Wang, W.-L., Wu, Q.-Y., Huang, N., Wang, T., Hu, H.-Y., 2016a. Synergistic effect between UV and chlorine (UV/chlorine) on the degradation of carbamazepine: influence factors and radical species. Water Res. 98, 190–198.

Wang, Y., Shen, C., Li, L., Li, H., Zhang, M., 2016b. Electrocatalytic degradation of ibuprofen in aqueous solution by a cobalt-doped modified lead dioxide electrode: influencing factors and energy demand. RSC Adv. 6 (36), 30598–30610.
Vasiliadou, I., Molina, R., Martínez, F., Melero, J., 2014. Experimental and modeling study on removal of pharmaceutically active compounds in rotating biological contactors. J. Hazard. Mater. 274, 473–482.
Wang, W., Lu, Y., Luo, H., Liu, G., Zhang, R., Jin, S., 2018. A microbial electro-Fenton cell for removing carbamazepine in wastewater with electricity output. Water Res. 139, 58–65.
Werner, C.M., Hoppe-Jones, C., Saikaly, P.E., Logan, B.E., Amy, G.L., 2015. Attenuation of trace organic compounds (TOrCs) in bioelectrochemical systems. Water Res. 73, 56–67.
Wols, B., Hofman-Caris, C., Harmsen, D., Beerendonk, E., 2013. Degradation of 40 selected pharmaceuticals by UV/H2O2. Water Res. 47 (15), 5876–5888.
Wu, J., Cagnetta, G., Wang, B., Cui, Y., Deng, S., Wang, Y., Huang, J., Yu, G., 2019. Efficient degradation of carbamazepine by organo-montmorillonite supported nCoFe2O4-activated peroxymonosulfate process. Chem. Eng. J. 368, 824–836.
Xiang, Y., Fang, J., Shang, C., 2016. Kinetics and pathways of ibuprofen degradation by the UV/chlorine advanced oxidation process. Water Res. 90, 301–308.
Xu, J., Li, L., Guo, C., Zhang, Y., Meng, W., 2013. Photocatalytic degradation of carbamazepine by tailored BiPO4: efficiency, intermediates and pathway. Appl. Catal. B Environ. 130, 285–292.
Yang, Y., Lu, X., Jiang, J., Ma, J., Liu, G., Cao, Y., Liu, W., Li, J., Pang, S., Kong, X., 2017. Degradation of sulfamethoxazole by UV, UV/H2O2 and UV/persulfate (PDS): formation of oxidation products and effect of bicarbonate. Water Res. 118, 196–207.
Yin, R., Guo, W., Wang, H., Du, J., Zhou, X., Wu, Q., Zheng, H., Chang, J., Ren, N., 2018. Enhanced peroxymonosulfate activation for sulfamethazine degradation by ultrasound irradiation: performances and mechanisms. Chem. Eng. J. 335, 145–153.
Yu, X., Zhou, M., Ren, G., Ma, L., 2015. A novel dual gas diffusion electrodes system for efficient hydrogen peroxide generation used in electro-Fenton. Chem. Eng. J. 263, 92–100.
Yuan, F., Hu, C., Hu, X., Qu, J., Yang, M., 2009. Degradation of selected pharmaceuticals in aqueous solution with UV and UV/H2O2. Water Res. 43 (6), 1766–1774.
Zhang, Y., Angelidaki, I., 2015. Recovery of ammonia and sulfate from waste streams and bioenergy production via bipolar bioelectrodialysis. Water Res. 85, 177–184.
Zhang, L., Yin, X., Li, S.F.Y., 2015a. Bio-electrochemical degradation of paracetamol in a microbial fuel cell-Fenton system. Chem. Eng. J. 276, 185–192.
Zhang, Y., Wang, Y., Angelidaki, I., 2015b. Alternate switching between microbial fuel cell and microbial electrolysis cell operation as a new method to control H2O2 level in bioelectro-Fenton system. J. Power Sources 291, 108–116.
Zhang, W., Zhou, S., Sun, J., Meng, X., Luo, J., Zhou, D., Crittenden, J., 2018. Impact of chloride ions on UV/H2O2 and UV/persulfate advanced oxidation processes. Environ. Sci. Technol. 52 (13), 7380–7389.
Zhang, B.-T., Wang, Q., Zhang, Y., Teng, Y., Fan, M., 2020. Degradation of ibuprofen in the carbon dots/Fe3O4@ carbon sphere pomegranate-like composites activated persulfate system. Sep. Purif. Technol. 116820.
Zhou, L., Hu, Z., Zhang, C., Bi, Z., Jin, T., Zhou, M., 2013. Electrogeneration of hydrogen peroxide for electro-Fenton system by oxygen reduction using chemically modified graphite felt cathode. Sep. Purif. Technol. 111, 131–136.
Zhou, Y., Wu, S., Zhou, H., Huang, H., Zhao, J., Deng, Y., Wang, H., Yang, Y., Yang, J., Luo, L., 2018. Chiral pharmaceuticals: environment sources, potential human health impacts, remediation technologies and future perspective. Environ. Int. 121, 523–537.
Zhu, S., Dong, B., Wu, Y., Bu, L., Zhou, S., 2019. Degradation of carbamazepine by vacuum-UV oxidation process: kinetics modeling and energy efficiency. J. Hazard. Mater. 368, 178–185.
Ziylan, A., Ince, N.H., 2011. The occurrence and fate of anti-inflammatory and analgesic pharmaceuticals in sewage and fresh water: treatability by conventional and non-conventional processes. J. Hazard. Mater. 187 (1–3), 24–36.
Zou, R., Angelidaki, I., Jin, B., Zhang, Y., 2020a. Feasibility and applicability of the scaling-up of bio-electro-Fenton system for textile wastewater treatment. Environ. Int. 134, 105352.
Zou, R., Tang, K., Angelidaki, I., Andersen, H.R., Zhang, Y., 2020b. An innovative microbial electrochemical ultraviolet photolysis cell (MEUC) for efficient degradation of carbamazepine. Water Res. 187, 116451.
Zou, R., Angelidaki, I., Yang, X., Tang, K., Andersen, H.R., Zhang, Y., 2020c. Degradation of pharmaceuticals from wastewater in a 20-L continuous flow bio-electro-Fenton (BEF) system. Sci. Total Environ. 727, 138684.
Zou, R., Tang, K., Hambly, A.C., Wünsch, U.J., Andersen, H.R., Angelidaki, I., Zhang, Y., 2022. When microbial electrochemistry meets UV: the applicability to high-strength real pharmaceutical industry wastewater. J. Hazard. Mater. 423, 127151.